

Advances in monolithic porous materials tailored in liquid media: around inorganic oxides and organic polymers

Kazuyoshi KANAMORI[†]

Department of Chemistry, Graduate School of Science, Kyoto University, Kitashirakawa, Sakyo-ku, Kyoto 606-8502, Japan

This review briefly surveys, with an emphasis on the author's works, porous monoliths tailored by liquid-phase synthesis. Porous structures ranging from mesopore to macropore regions are induced in sol-gel polymerizing systems, which yield various porous materials such as inorganic oxides, organic-inorganic hybrids, crosslinked polymers, and carbons. It should particularly be noted that the networks must be homogeneous enough to obtain monolithic materials with fine pore structures, and for this purpose, the chemical reactions must be carefully designed and controlled. With exemplifying alkoxy-derived sol-gel systems and controlled/living radical polymerization systems, pore formations and applications of resultant materials are demonstrated.

©2012 The Ceramic Society of Japan. All rights reserved.

Key-words : Porous material, Sol-gel, Inorganic oxide, Organic-inorganic hybrid, Crosslinked polymer and carbon

[Received September 28, 2011; Accepted October 14, 2011]

1. Introduction

Porous materials are important platform for state-of-the-art key technologies such as adsorption, separation, filtration, sensors, drug delivery and energy storages.¹⁾⁻⁶⁾ Size, volume and shape of the pores, chemical composition of the matrix, and materials shapes are primal parameters that have to be controlled to meet the requirements in specific applications. Among processes to fabricate porous materials, the liquid-phase process, which involves reactions of the precursors and pore formations in liquid media, has been the most widely studied because of its versatility, simplicity and mild reaction conditions. The so-called sol-gel process is the representative strategy to obtain porous materials in particles, films, and monoliths. It typically undergoes the transition from solution in which starting components are completely dissolved, via the "sol" state, i.e. liquid with colloidal dispersion, and to the "gel" state which is the solid incorporated with liquid.⁷⁾ A wide variety of pore structures is induced during this process within the gelling matrix.

We have been strongly interested in porous materials, especially monoliths, prepared by liquid-phase processes with a firm idea that it is crucial to make homogeneous networks to tailor well-defined pore structures. This is attributed to the simple fact that it is impossible to induce a porous structure within a network with the heterogeneity coarser than the intended structure. In other words, the intrinsic heterogeneity in a network should be kept finer than the intended porous structure. Various well-defined porous materials such as aerogels, ordered mesoporous, and macroporous materials are designed under such condition. Fortunately, this condition is unconsciously satisfied in the alkoxy-derived silica sol-gel systems. In most conditions in the silica sol-gel system, one can readily obtain a monolithic transparent gel from tetraalkoxysilane, owing to the stepwise reaction of the alkoxy-silanes without abruptly forming "too-large" condensates which should inhomogeneously segregate from the solution or networks. Although the heterogeneous

networks can be used to obtain macroporous materials as mentioned later (section 4), it is difficult to control the pore properties because of the stochastic and unpredictable behavior.

In addition to the silica system, which has been the basis of abovementioned porous materials, fine and well-defined pore structures can also be imparted in other siloxane-based systems starting from organotrialkoxysilanes, bridged bisalkoxysilanes, etc. As examples, we will show flexible aerogels and xerogels and macroporous monoliths prepared from organotrialkoxysilane in section 2. However, one should be careful for the homogeneity of the networks in other oxide systems; homogeneous (transparent) monolithic gels are difficult to obtain due to the high reactivity of metal alkoxides. We have also developed a simple and easy way to prepare homogeneous networks in the alkoxy-derived titania system, which can be utilized to the preparation of macroporous titania monoliths (section 3). We also utilized homogeneous networks formed by controlled/living radical polymerization⁸⁾ for the development of macroporous crosslinked polymer monoliths, which can also be converted into carbon materials with high specific surface area by carbonization and activation (section 4). Some possible applications for these new porous monoliths are also demonstrated.

Since we have recently published some reviews on the progresses of porous organic-inorganic hybrids and crosslinked polymers,⁹⁾⁻¹²⁾ we will just give a concise picture on these issues in the current review. Specifically, note that sections 2 and 4 are largely based on these previous reviews.

2. Flexible organic-inorganic hybrid aerogels and xerogels

2.1 Preparation

Aerogels¹³⁾⁻¹⁷⁾ are a particular class of low density porous solids characterized by their high porosity (~90%). Amongst a wide variety of available chemical compositions, silica aerogels are particularly important for unique properties such as high visible-light transparency (typically ~90%), low density (~0.1 g cm⁻³), low refractive index, low dielectric constant, etc. More importantly, silica aerogels show extremely low thermal conductivity (<10 mW m⁻¹ K⁻¹), which is the lowest among all

[†] Corresponding author: K. Kanamori; E-mail: kanamori@kuchem.kyoto-u.ac.jp

solids.¹⁸⁾ This excellent thermal insulation property is expected to help more efficient use of fuel energies and to save natural resources. However, a special drying process utilizing supercritical fluid is required to preserve significantly tenuous pores when making as-prepared wet gels into aerogels. This fact increases the production cost and hampers the extended applications of aerogels. In addition, since hydrophilic surfaces of bare silica aerogels are not stable in a humid condition, a hydrophobizing process using a coupling agent such as hexamethyldisilazane (HMDS) is needed.¹⁹⁾

We have prepared mechanically strong and flexible aerogels with high transparency and low density by preparing aerogels with an organic-inorganic hybrid composition. We used methyltrimethoxysilane (MTMS) as the precursor and the ideal product obtained from MTMS is methylsilsesquioxane (MSQ, $\text{CH}_3\text{SiO}_{1.5}$). Gels based on the random networks of MSQ should be termed as polymethylsilsesquioxane (PMSQ). To avoid the extended cyclization and phase separation,¹⁰⁾ we employed an acid-base two-step reaction. Acid-catalyzed hydrolysis is promoted in the first step, followed by enhanced base-catalyzed polycondensation in the second step, where pH increase is caused by the in-situ hydrolysis of urea. In addition, appropriate surfactant is used to suppress macroscopic phase separation. This is a modified two-step process which can be performed as a one-pot reaction. With appropriate surfactant, such as *n*-hexadecyltrimethylammonium salt (CTAB for bromide or CTAC for chloride) or poly(ethylene oxide)-*block*-poly(propylene oxide)-*block*-poly(ethylene oxide) triblock copolymers, phase separation is effectively suppressed and transparent aerogels can be obtained.²⁰⁾

The PMSQ aerogels obtained after supercritical drying exhibit similar properties to the carefully-prepared conventional silica aerogels such as low density ($<0.15 \text{ g cm}^{-3}$) and high porosity ($\sim 90\%$), and high visible-light transparency ($\sim 90\%$ at 550 nm through a 10 mm-thick-equivalent sample).²⁰⁻²²⁾ The typical PMSQ aerogels prepared with CTAB consist of a well-defined mesoscopic pore structure with 30–50 nm pores and solid frameworks formed by nano particles ($\sim 10 \text{ nm}$ in diameter). Owing to the methyl groups, the PMSQ aerogels naturally exhibit hydrophobicity without the surface modification. Thus, the structure and properties, except for hydrophobicity and mechanical properties, of PMSQ aerogels are almost the same as silica aerogels.

2.2 Mechanical properties and aerogel-like xerogels

The major advantage in PMSQ aerogels is the flexible and elastic nature upon compression. The aerogel prepared with an optimal condition can be uniaxially compressed up to 80% without cracking, followed by recovering the original size and shape upon unloading, showing the sponge-like compression-reexpansion behavior (spring-back). Although some researchers observed spring-back of silica aerogels treated with a hydrophobic coupling agent such as trimethylchlorosilane,^{23,24)} this is the first example showing the large-scale spring-back in a transparent aerogel monolith. This is attributed to the unique structural characteristics in the PMSQ networks; the lower crosslinking density offers softness, the lower residual silanol groups prohibit irreversible shrinkage upon compression, and the highly concentrated methyl groups induce spring-back by repulsing each other.

It is well recognized that costly supercritical drying is the high barrier for the aerogel production. Much effort has therefore been

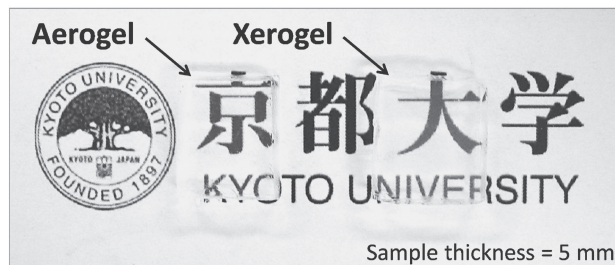
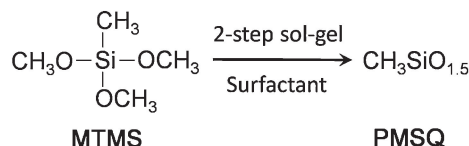


Fig. 1. Comparison between supercritically-dried PMSQ aerogel and evaporatively-dried PMSQ xerogel with similar pore properties.

paid to obtain aerogels without relying on supercritical drying, i.e. evaporative drying at ambient pressure. Translucent hydrophobic silica aerogel granules prepared by ambient pressure drying can be commercially available; however, virtually no other examples are found in monolithic aerogels with high transparency and porosity. The essential reason is that compressive strength of rigid and fragile silica aerogel is lower than the applied compressive stress during ambient pressure drying.^{25,26)} Another reason arises from the fact that a high concentration of silanol (Si-OH) groups reacts with each other to form new siloxane bonds when compressed. This cannot be completely avoided even with the surface-treated silica, and results in irreversible shrinkage during drying in many cases.

The flexible nature of PMSQ aerogels facilitates elastic deformation during drying. In an optimized condition, the drying gels do not crack owing to the high compressive strength and spring-back to the original size and shape after pores become empty even without the surface modification. Xerogels with almost the same properties as aerogels can be successfully obtained after careful evaporative drying using a drying solvent with low surface tension. **Figure 1** compares aerogel obtained by supercritical drying and xerogel by ambient pressure drying prepared from the same starting composition. Values of bulk density are comparable (0.13 g cm^{-3} for aerogel and 0.14 g cm^{-3} for xerogel) and those of visible light transmittance are also comparable between the aerogel and xerogel. We also confirmed that thermal conductivity of the PMSQ xerogel is as low as silica aerogel with the similar density at ambient pressure ($\sim 13 \text{ mW m}^{-1} \text{ K}^{-1}$). Large PMSQ xerogel tiles with the size of $250 \times 250 \times 10 \text{ mm}^3$ are readily available with a good reproducibility. The more extended applications of the PMSQ xerogels to thermal insulating materials are highly expected when the low-cost industrial production process will be established without using supercritical drying.

2.3 Porous materials derived from the PMSQ aerogel system

Utilizing the urea-assisted acid-base two-step process containing surfactant, two other types of porous materials have been derived. The first example is the PMSQ monoliths with well-defined macropores (**Fig. 2**),²⁷⁾ which are regulated by spinodal decomposition occurring in parallel with the sol-gel transition (the phase separation method).^{28,29)} With decreasing surfactant (Pluronic F127 in this case), a transition from the transparent mesoporous aerogel to opaque macroporous gel was observed.

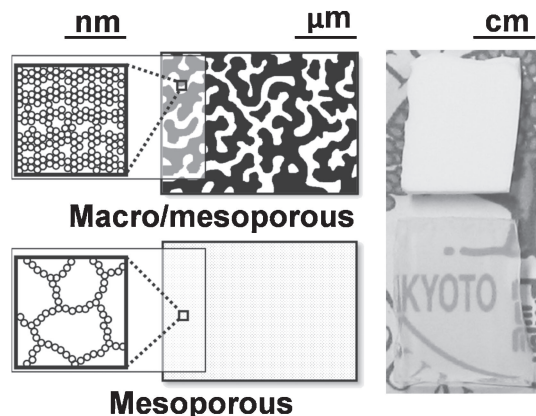


Fig. 2. Transparent mesoporous PMSQ monoliths and hierarchically porous structure of PMSQ monoliths prepared with varied concentrations of surfactant (Pluronic F127).

The important feature in this material is that mesopores around 10 nm in size and $0.2\text{--}0.4\text{ cm}^3\text{ g}^{-1}$ in volume with BET specific surface area $>400\text{ m}^2\text{ g}^{-1}$ are included in the skeletons of macropores. In our previous results on macroporous PMSQ monoliths prepared using the one-step strong acid-catalyzed systems,³⁰ we did not find any mesopores in the macropore skeletons. In the polymeric network resulted from the acid-catalyzed system, together with the relatively high volume fraction of monomers [for the MTMS-methanol-water system, volume fraction of MTMS/(entire sol) is typically ~ 0.7], no mesopores are formed in the phase-separated gelling phase. By the base-catalyzed condensation, on the other hand, highly branched colloid-like polymers form as a result of the more vigorous condensation into more-branched silanol species, resulting in inter-particles mesopores formed in the colloidal networks. To the best of our knowledge, this is the first example on hierarchically porous PMSQ monoliths with well-defined macropores, and we believe that this system serves as a good basis for the better control of mesopores in PMSQ monoliths, which may lead to applications to separation media with improved performances.

The second example is superflexible porous monoliths from a mixture of MTMS and dimethyldimethoxysilane (DMDMS).³¹ With increasing DMDMS/MTMS molar ratio, though the gels become opaque due to the enhanced hydrophobicity of the networks, resultant gels become more and more flexible and bendable as shown in Fig. 3. The stress upon 80% compression can be down to ca. 0.05 MPa, which is 1/100 of the MTMS-derived aerogel. These “marshmallow-like” gels with typical bulk density $\sim 0.10\text{ g cm}^{-3}$ can be obtained via ambient pressure

drying, and can be subjected to repetitive wetting and drying. Since these bendable gels exhibit good sound absorption properties, applications to high-performance acoustic insulators can be expected.

3. Porous Titania monoliths

3.1 Our strategy to prepare homogeneous networks

It is well known that metal alkoxides (i.e. except for silicon alkoxide) generally shows very high reactivity, and therefore the monolithic gel formation from these alkoxides is difficult. This is predominantly attributed to the large difference of electronegativity between the alkoxide group and metal, and the ability of the metal to take more than one oxidation states.³² In the case of titanium(IV) alkoxide, the titanium is highly susceptible to the attack of nucleophiles such as water to fulfill the most stable hexacoordination state. Moreover, the large difference of electronegativity induces large positive partial charge on the titanium, which makes more reactive against nucleophiles. As a result of the rapid and uncontrollable hydrolysis and condensation reactions, precipitates rather than monoliths are the resultant product in many of the titania sol-gel systems. In order to exploit their unique properties represented by high refractive index and photocatalytic activities, a fine tuning of internal structures as well as material shapes is required by controlling the reactions of titanium precursors.

Yoldas et al. used a strong acid and a small amount of water to obtain monolithic titania gels.³³ The strong acid protonates the alkoxy groups, which makes alkoxy groups a good leaving group and enhances hydrolysis. The protonated hydroxyl groups in the hydrolyzed species more or less hinder the additional nucleophilic attack to the titanium, which retards polycondensation. In addition, the titania oligomers and polymers are stabilized by the electrostatic repulsion by the positive surface charge. All these effects deaccelerate polycondensation over hydrolysis, and thus contribute to the formation of clear monolithic titania gels. Other strategies to reduce the reactivity employ the chelating agents such as β -diketones^{7,32} to stabilize the monomer by coordinating to the titanium, or gradually supplying water as the by-product of esterification of acid and alcohol.³⁴

The outstanding progress for homogeneous network formations of metal oxides was established by Itoh et al.³⁵ and Gash et al.³⁶ from ionic precursors, in which hydrated metal ions undergo hydrolysis and condensation under the co-presence of a proton scavenger. A stable metal salt is dissolved in water to form aqua complex, and subsequent addition of an epoxide (the proton scavenger, such as propylene oxide) consumes protons from the acidic hydrated metal, which promote further hydrolysis and ololation/oxolation-based polycondensation under an increasing

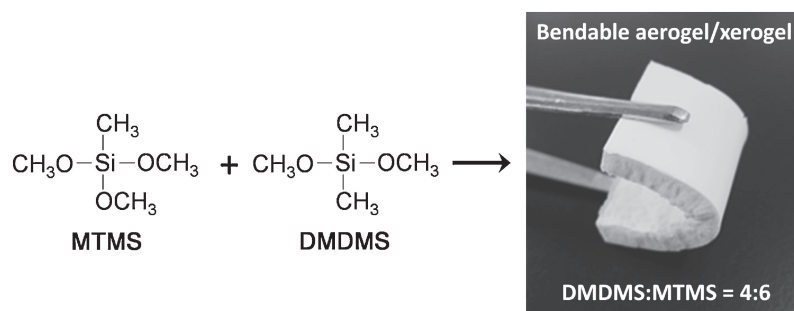


Fig. 3. Flexible aerogel/xerogel prepared from DMDMS/MTMS co-precursors exhibiting a bendable feature. By increasing the DMDMS ratio, the compressive stress dramatically decreases to ca. 1/100 of MTMS-derived aerogels.

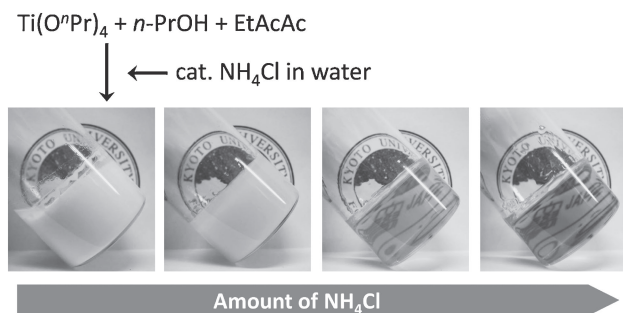


Fig. 4. Reaction scheme and appearance of transparent monolithic titania gels. The simple procedure employing chelating agent and mineral salt in a mild condition gives titania monoliths. (From left to right) $\text{NH}_4\text{Cl}/\text{Ti} = 0, 0.0025, 0.0050, \text{ and } 0.0075$ in molar ratio.

pH condition. When the pH exceeds the pH-dependent solubility curve of the metal oxo-hydroxides, the polymerizing species simultaneously precipitate and interconnect to form monolithic gels. Various monolithic gels composed of metal (Al, Fe, Zr, Cr, Ga, Sn, etc.) oxides have been reported.³⁷⁾ However, only a few applications of this technique to the monolithic titania systems are found³⁸⁾ presumably because stable titanium salt precursors are rather uncommon. In addition, the monolithic gel formation is relatively difficult because titanium species start to precipitate at a strongly acidic condition (pH ~ 1 – 2).

We have developed a unique strategy to obtain transparent titania monoliths by the combination of chelating agent and mineral salt.³⁹⁾ Since this process requires no acidic or basic catalyst, titania monolithic gels can be easily obtained in a mild condition. Titanium(IV) alkoxide is firstly stabilized with a chelating agent such as ethyl acetylacetonate (EtAcAc) in alcohol, followed by an addition of the aqueous solution of catalytic amount of a mineral salt. Subsequent gelation at 40°C gives transparent monoliths. The most effective parameters are concentration and kind of the salt additive. After the investigation of various mineral salts, we have concluded that the salts containing strong acid anions such as Cl^- , Br^- , I^- , NO_3^- must be employed while no preferences are found in cations; NH_4^+ , K^+ , Ca^{2+} , Al^{3+} , Fe^{3+} , Y^{3+} , La^{3+} and Ce^{3+} are confirmed to work. With increasing concentration of salt (NH_4Cl in this case) from 0 to 0.75 mol % with respect to titanium alkoxide, the resultant gels become more transparent as shown in Fig. 4 (note that only an opaque gel can be obtained without the salt). The proposed reaction mechanism is as follows. Under the co-presence of water, the anions coordinate to the (favorably more hydrolyzed or branched) titanium to satisfy the hexacoordination state using lone pairs, and suppress the reactivity. The high electronegativity of the anions contributes to the effective coordination. However, this in turn makes the bond between titanium and anion more ionic. The anions should dissociate after a certain period of time, and dissociated anions diffuse to another titanium to suppress the reactivity of the site. As a result, the whole hydrolysis and polycondensation process becomes moderate, and homogeneous networks rather than precipitation or inhomogeneous gels are fabricated in such a facile way. This protocol can be extended to obtain various porous materials such as those demonstrated in the silica sol-gel system, because the homogeneous titania networks can play as the matrix where fine porous structures are induced. In the succeeding section, we will show macroporous titania monoliths as an instance prepared by combining this protocol with the phase separation method.

Hierarchically porous TiO_2 (anatase) monolith

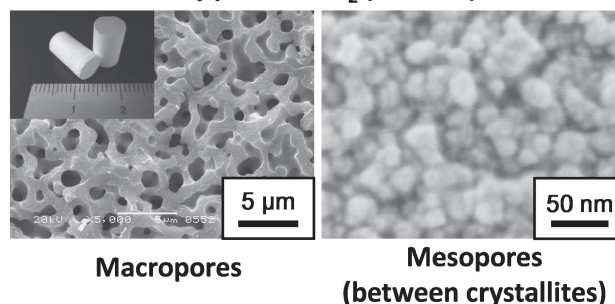


Fig. 5. Hierarchically porous titania monoliths obtained by the chelate and salt method. Co-presence of PEO induces phase separation to form well-defined macropores. Mesopores correspond to the interstices in-between the crystallites.

3.2 Macroporous titania monoliths and their applications

Well-defined macroporous titania monoliths have been obtained utilizing the homogeneous network formation described above (Fig. 5).⁴⁰⁾ Macroscopic phase separation is induced in the homogeneous networks by employing poly(ethylene oxide) (PEO). The phase-separated structure coarsens with increasing amount of PEO, resulting in a controllability of pore size from submicrons to $\sim 10 \mu\text{m}$. The as-prepared amorphous titania turns into anatase through the stepwise solvent-exchange process from ethanol to water at 60°C , during which the chelating agent in parallel decomposes by hydrolysis and decarbonation. The anatase crystallites become larger with increasing calcination temperature, and finally transform to the rutile phase at 700°C . The mesopores are embedded as the interstices of the crystallites, configuring the hierarchically porous structure. The interstices disappear when the rutile phase develops at 700°C . Compared to the previous methods utilizing colloidal precursors⁴¹⁾ or strong acid,⁴²⁾ the present process takes advantage in terms of the mild condition and monolithicity of the product.

The titania monoliths were tested as the separation media for high-performance liquid chromatography (HPLC). Since titania exhibits selective adsorption of organophosphates,^{43,44)} monolithic titania columns are regarded as the first candidate of efficient separation media for biomaterials especially in the medical and biological fields. We,⁴⁵⁾ as well as Konishi et al.,⁴⁶⁾ have successfully demonstrated that monolithic titania with the hierarchically porous structure is effective for the separation of phosphates such as adenosine 5'-monophosphate (AMP), adenosine 5'-diphosphate (ADP), and adenosine 5'-triphosphate (ATP). Whereas the separation efficiency of these monolithic columns does not reach the commercial particle-packed column, we believe that more intensive study will improve column performances.

The chemical compositions of titania monoliths have been extended to several metal titanates such as $\text{MgTi}_2\text{O}_5/\text{MgTiO}_3$, CaTiO_3 , SrTiO_3 , and BaTiO_3 .^{47,48)} A simple procedure of impregnation of desired metal cations in the titania monoliths during the solvent exchange process results in the metal carbonate/titania monolithic composites. The carbonates are precipitated by the reaction between cations and carbon dioxide, which were generated by the hydrolysis of urea incorporated in the exchanging solution as well as by the hydrolysis-decarbonation of the chelate (EtAcAc). Subsequent calcination at $< 1000^\circ\text{C}$ induces solid-state reactions of carbonates and titania matrix to give metal titanates, as exhibited in Fig. 6 for

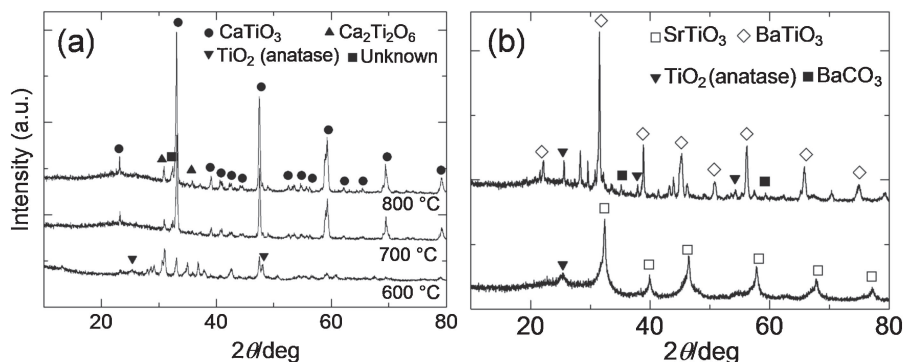


Fig. 6. Powder XRD profiles of perovskite monoliths obtained from titania monoliths shown in Fig. 5, by impregnating cations such as Ca²⁺, Sr²⁺, and Ba²⁺. (a) Growth of CaTiO₃ perovskite structure with increasing calcination temperature. (b) Samples with different perovskite structures (SrTiO₃ and BaTiO₃) calcined at 800 °C.

perovskites. Since these mixed metal oxide monoliths possess potential applicability with unique electronic and magnetic properties, further research is desired.

4. Porous organic crosslinked polymer and carbon monoliths

4.1 Porous materials from organic polymer gel systems

Porous organic crosslinked polymers are fascinating materials which can be used for separation media, catalyst supports, and carbon sources. In particular, the polymers applied to chromatographic separation media are often simply called as “polymer monoliths” and mainly prepared using free radical polymerization of monomers containing multiple vinyl groups in a solvent.^{49),50)} Co-precursor systems consisting of mono-vinyl and di-vinyl compounds such as styrene-divinylbenzene are often employed. Monolithic separation media especially for high molecular weight compounds such as proteins and polypeptides are successful applications because of the presence of micrometer-sized macropores and of the absence of mesopores which disturb the elution of such large molecules. However, polymer monoliths suffer from difficulties in controlling pore properties, e.g. pore size and pore volume, which are major parameters determining separation performances.

The reaction mechanism in free radical polymerization is predominantly responsible for the lack of controllability of pores in polymer monoliths. In the free radical polymerization mechanism, remarkably unstable and reactive free radicals generated from initiator (I) such as 2,2'-azobisisobutyronitrile (AIBN) and benzoyl peroxide (BPO) cleave the double bond in vinyl monomers, generating monomer radicals (M•). The monomer radicals are also reactive and several parallel reactions including propagation, chain transfer and termination occur in an uncontrolled way. In the crosslinking systems, hence, the monomers once started to react will grow in a large size by intra- or intermolecular crosslinking within a short time, resulting in the formation and segregation of “microgels” or globules from the solvent. Since the length scale of the microgels is in the order of micrometers, macropores in-between microgels are stochastically formed in the course of gelation. In such systems, a fine control of the macropores is appreciably difficult.

In controlled/living radical polymerization (CRP),⁵¹⁾ undesirable chain transfer and termination reactions are highly suppressed by employing a chemical agent (X) which reversibly attaches to the growing end (P•) and stabilizes it as the “domant” (P-X) as shown in Fig. 7. The domant and dissociated states

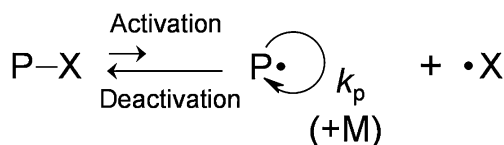


Fig. 7. General concept of controlled/living radical polymerization; M, P, and X show monomer, polymer, and a chemical agent which attaches the growing end and makes “domant” species (P-X). Monomers are inserted to increase molecular weight on the “activation” of the equilibrium.

(P• + X) are in equilibrium with considerably low radical concentrations, that is, the equilibrium is mostly balanced on the former. By applying energy for dissociation by heat or light, the equilibrium moves to the latter, and monomer is inserted to forward the propagation reaction during dissociation. The undesired chain transfer and termination reactions are effectively suppressed by the low radical concentration, resulting in polymeric products with a narrow molecular weight distribution. Since the growing end is still active or “living” when all the monomers are consumed, well-defined polymers with unique structures such as block and graft copolymers are readily obtained by appending different monomer(s) to the reacted system. Several types of CRP are proposed based on different reaction mechanisms.⁵²⁾⁻⁵⁶⁾ Versatility of applicable monomers and reaction conditions are dependent on the mechanisms.

In the crosslinking systems reacted by living polymerization, more homogeneous and uniform networks are reported to form.^{57),58)} Conversion of the vinyl groups gradually increases with reaction time, and crosslinking density also increases with conversion, leading to the homogeneous networks. The living character offers the narrow molecular weight distribution, sufficient chain/network relaxation, and reactant diffusion in the system. These aspects avoid the formation of microgels, leading to the more homogeneous networks.

4.2 Macroporous crosslinked polymer monoliths

While the heterogeneous networks derived by free radical polymerization are utilized to prepare macroporous “polymer monoliths” as mentioned above, we employed CRP to induce spinodal decomposition in the gelling networks and prepare well-defined macroporous monoliths with controllable porosity. Spinodal decomposition is induced in a homogeneous network under the co-presence of nonreactive chain polymer, which induces entropy-driven instability with the progress of polymerization of monomer(s) and does not participate in the network.

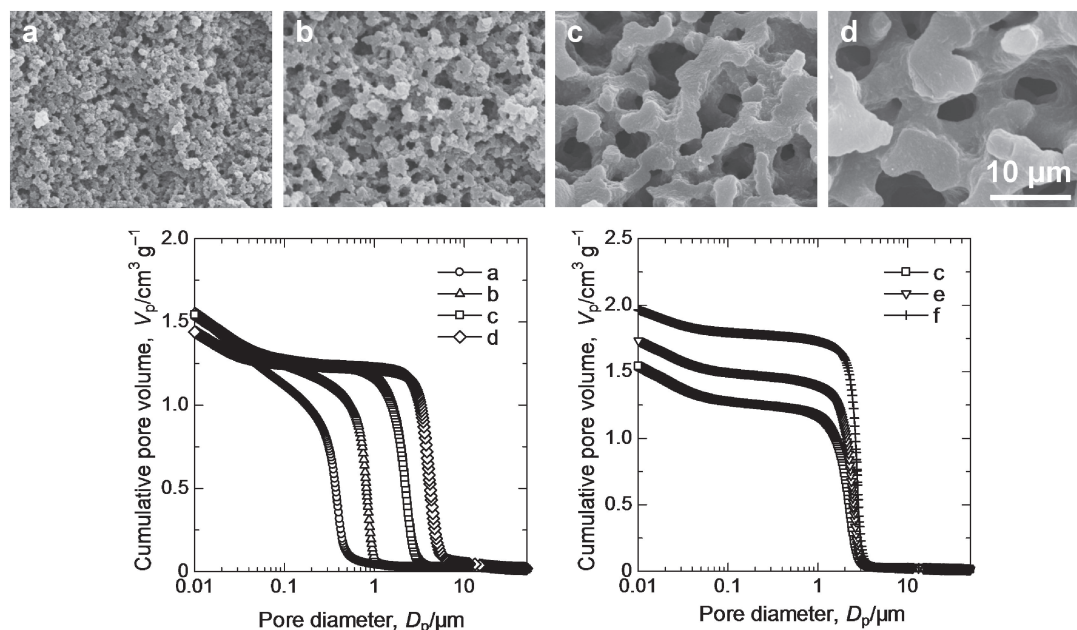


Fig. 8. Typical macroporous morphologies of PDVB monoliths prepared by NMP. From parts a to d, macropores are coarsened with increasing concentration of PDMS. The lower figures obtained by mercury porosimetry demonstrates that only macropore size can be varied with increasing PDMS (from a to d), and only macropore volume can be changed with increasing both PDMS and TMB (solvent) (c, e, and f).

As the typical starting composition, divinylbenzene (DVB), 1,3,5-trimethylbenzene [good solvent for DVB and poly(divinylbenzene) (PDVB)] and nonreactive polymer such as poly(dimethylsiloxane) (PDMS) to induce phase separation, are mixed with an initiator (I)/promoter (X) system of CRP. In the case of nitroxide-mediated polymerization (NMP), AIBN or BPO and commercially-available stable radical 2,2,6,6-tetramethyl-1-piperidinyloxy (TEMPO) are used as the initiator/promoter system. The organotellurium-mediated living radical polymerization (TERP) system uses ethyl-2-methyl-2-butyltellanyl propionate (BTEE) with or without the radical initiator. The mixture undergoes CRP at elevated temperatures at 70–125°C depending on the CRP system, resulting in well-defined macroporous PDVB monoliths as shown in **Fig. 8**. The macroporous morphology coarsens with the increasing amount of PDMS (from a to d), and the macropore size and volume are independently controlled by changing the starting composition, which had been difficult by free radical polymerization. In addition, smaller pores in the nanometer scale (with a wide size distribution up to ca. 100 nm) are found inside the macropore skeletons by the nitrogen adsorption–desorption measurement. The monoliths therefore possess hierarchically pore structures with relatively high specific surface area ($\sim 600\text{--}800\text{ m}^2\text{ g}^{-1}$).

So far, we have obtained several macroporous cross-linked polymers from DVB,^{59,60} glycerol 1,3-dimethacrylate (GDMA),^{61,62} trimethylolpropane trimethacrylate (Trim)⁶² and *N,N'*-methylenebisacrylamide (BIS)⁶³ in the CRP systems such as NMP, TERP, and atom transfer radical polymerization (ATRP) as depicted in **Fig. 9**. We have also confirmed that the similar porous materials can be obtained by anionic polymerization, which also behaves as living polymerization, using such as *n*-butyl lithium or potassium *tert*-butoxide. Again, the formation of network without heterogeneity coarser than the desired structure is the most crucial factor to obtain porous materials. The gradual or stepwise increase of crosslinking density with

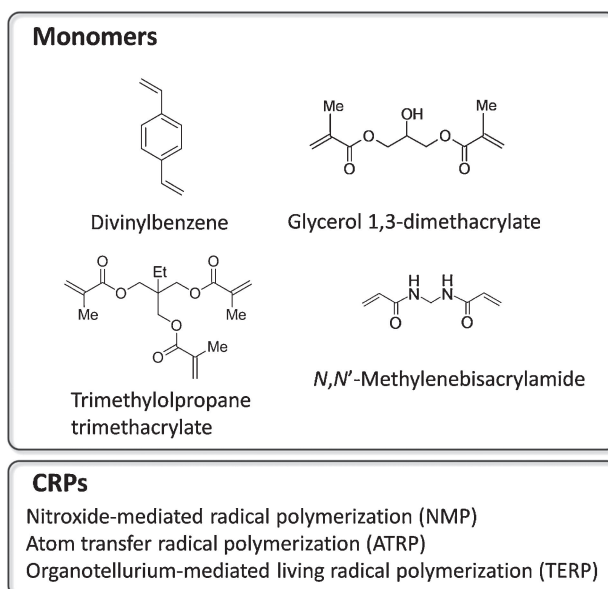


Fig. 9. Monomers and polymerization techniques examined so far. We believe any living polymerization systems including anionic and cationic initiated by heat or radiation can be used to tailor well-defined macroporous monoliths.

conversion/reaction time is the essential feature to obtain homogeneous networks.

Although all of these examples are initiated and reacted by applying heat to the system, we have confirmed that the similar pore formations occur in the systems initiated by ultraviolet (UV) light irradiation as well. The UV-initiating system can offer a position-selective formation of porous parts for catalytic reaction, separation and purification in microfluidic channels of lab-on-a-chip devices, etc.^{64–66}

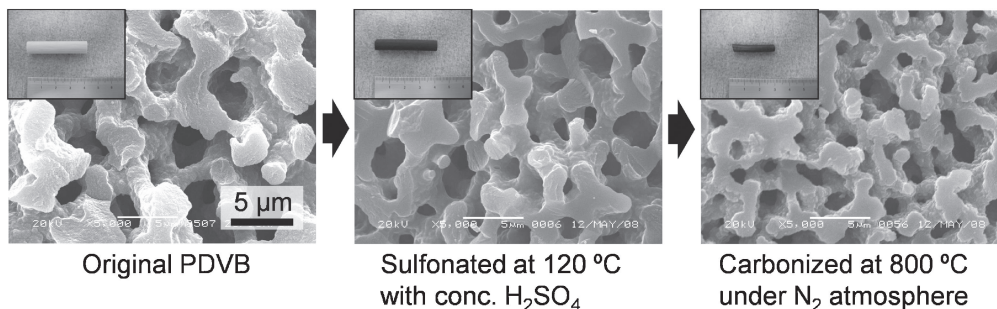
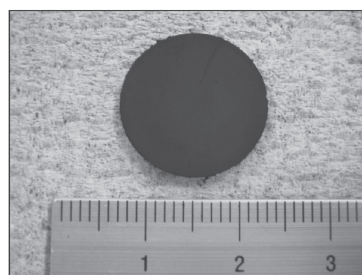


Fig. 10. Changes in appearance and morphology of PDVB monoliths by sulfonation and carbonization. Well-defined macropores and monolithicity are successfully preserved after carbonization.



Micro-/meso-/macroporous
Specific surface area : $2420 \text{ m}^2 \text{ g}^{-1}$
Bulk density : 0.22 g cm^{-3}

175 F g^{-1} (at 5 mV s^{-1})
 206 F g^{-1} (at 0.5 A g^{-1})

*in $2 \text{ M H}_2\text{SO}_4$ aq, three-electrode cell

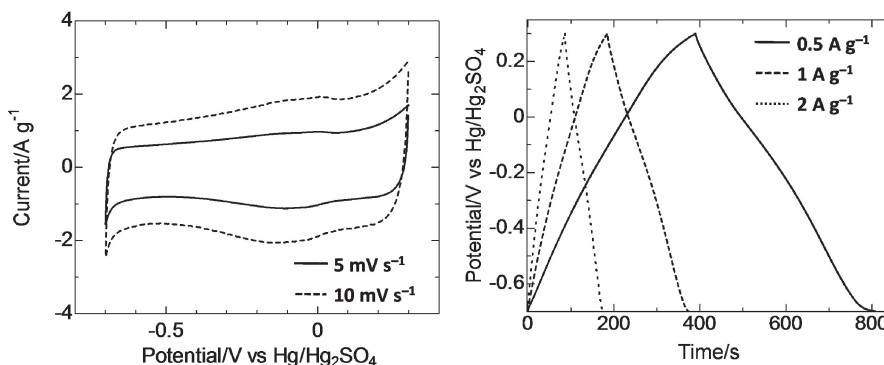


Fig. 11. Appearance of the typical activated carbon monoliths for the monolithic polarizable electrode. From electrochemical measurements such as cyclic voltammetry (CV, lower left) and galvanostatic charge–discharge (lower right), the high specific capacitance was confirmed, which, together with the monolithic feature, is advantageous for applications to electric double-layer capacitors.

4.3 Carbonization and application

The obtained PDVB monoliths can be converted to carbonaceous materials by carbonization in an inert atmosphere with preserving the macroporosity and monolithicity as shown in Fig. 10.^{67,68} Carbonization of as-prepared PDVB monoliths decreased the sample weight to 10–20% by the pyrolysis of the networks, and specific surface area drastically increased ($\sim 1500 \text{ m}^2 \text{ g}^{-1}$) by carbonization at $>900^\circ\text{C}$. The turbostratic structure, which is the disordered stacking of polycyclic aromatic (graphene) sheets, is proposed from the XRD patterns with broad peaks at around 23 and 43 deg, and the structure has been developed mainly at $600\text{--}800^\circ\text{C}$ confirmed by FTIR. Activation under 10% carbon dioxide in nitrogen further increases specific surface area above $2300 \text{ m}^2 \text{ g}^{-1}$. Sulfonation of as-prepared PDVB monoliths before carbonization suppresses the excess pyrolysis and carbon yield reaches 30–40%, because aromatic rings are bridged with sulfonyl groups at around 300°C in the course of carbonization.⁶⁹ At the same time, the pyrolyzing networks are mechanically reinforced by the sulfonyl bridges, which preserves nanometer-scaled pores in the original skeletons

from shrinkage. Hence, carbonization/activation of the sulfonated PDVB networks allows the development of micropores with preserving macro- and mesoporosity and monolithicity, resulting in hierarchically porous carbon monoliths with trimodal sizes of pores and increased specific surface area.

The activated carbon monoliths prepared from PDVB were electrochemically evaluated as a monolithic polarizable electrode. As shown in Fig. 11, specific capacitance was obtained such as 175 F g^{-1} at 5 mV s^{-1} [from cyclic voltammetry (CV)] and 206 F g^{-1} at 0.5 A g^{-1} (from galvanostatic charge–discharge) in 2 M aqueous H_2SO_4 using a three-electrode cell.⁷⁰ While conventional electrodes are typically fabricated in pellets or slurries from composites of activated carbons as active material, carbon black as conducting agent, and polymer binders, the monolithic electrode consists only of the active material with the hierarchical porosity. Therefore the effective diffusion and permeation of the electrolyte are expected and electric conductivity of the monoliths is relatively high owing to the continuous skeletal structure. Since the chemical and mechanical durabilities are also expected to be higher in the simple monolithic electrode,

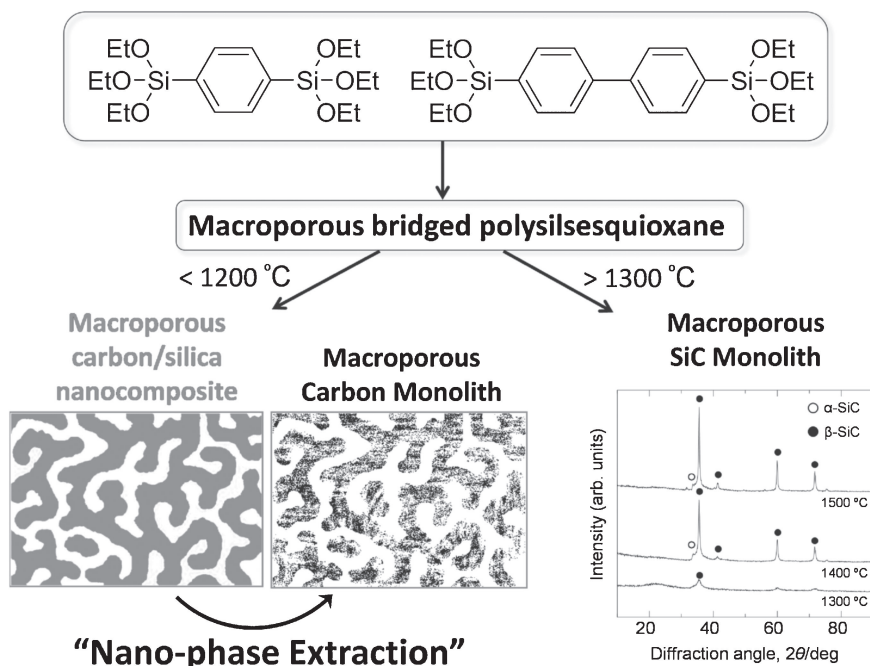


Fig. 12. A scheme for various porous materials derived from bridged bisalkoxysilanes. The controlled sol-gel process yields well-defined macroporous bridged polysilsesquioxanes, which can be converted to carbon/silica nanocomposite, carbon, and silicon carbide (SiC) monoliths with preserved macropores by the different post treatments.

applications are expected to polarizable electrodes for electric double-layer capacitors (EDLC) with a good reproducibility and cycle performance.

The (activated) carbon monoliths are also obtained by carbonization of macroporous phenolic resins,⁷¹⁾ employing sacrificial templates,^{72),73)} and removing silica phase from carbon/silica composites.⁷⁴⁾ We have also successfully obtained macroporous polysilsesquioxane monoliths from phenylene- and biphenylene-bridged alkoxy silanes for the first time, which can be converted to a carbon/silica nanocomposite monolith when heat-treated in inert atmosphere below 1200°C⁷⁵⁾ and silicon carbide (SiC) monoliths when heat-treated above 1300°C as shown in Fig. 12.^{76),77)} The nano-sized silica phase in the resultant carbon/silica nanocomposite can be removed using aqueous basic solution to increase micropores, typically ~ 1.5 nm,⁷⁸⁾ which we call the “nano-phase extraction” technique. Carbon monoliths with ~ 2000 m² g⁻¹ can be obtained by this method. Liu et al. also reported that ordered mesoporous silica in addition to carbon can be prepared by the removal of carbon phase by calcination in air from carbon-silica nanocomposite, which is obtained by parallel sol-gel reactions of silica and phenolic resins.^{79),80)} In spite of the expensive precursors in our approach, the single reaction system should be easier and obtainable pore properties would be more widely controllable. This new possibility for the source of carbon monoliths is expected to broaden the materials chemistry of carbons.

5. Conclusions and future perspectives

We have surveyed our recent progress in monolithic porous materials ranging from inorganics, hybrids, organic polymers, and to carbons. In particular, we have devoted our efforts to tailoring homogeneous networks, in which well-defined porous structures are induced especially by the phase separation technique. Some possible applications to separation media and electrochemical devices have also been demonstrated.

The research field of porous materials is the fast-evolving area, and various types of pores (size, volume and geometry) are explored over a wide range of chemical compositions. The recent advancement in porous materials has been further extending the properties and functionality, and a wide variety of applications in particular to energy-related materials such as electrode and hydrogen storage is rapidly developing. Recently, the thermal insulating abilities of aerogels are increasingly gathering attentions from the viewpoint of saving fuel energies. We believe the PMSQ aerogels become the first candidate to the insulating material for the next generation because these aerogels can achieve both high performance and a low cost for industrial productions. The carbon monoliths are also promising for the EDLCs, which may also contribute to the effective use of energy. The research on porous materials is surprisingly growing. We also have to extend our research to different types of porous materials to make a contribution to resolving the energy and environmental issues around the world. We expect new sophisticated materials out of the active research will help, support, and improve our lives for the future.

Acknowledgements The author wishes to thank all the co-workers who supported him, gave critical ideas to him, and contributed to his experimental works. Here the author cannot single all the names out, but most of the coworkers are listed as the co-authors in the references.

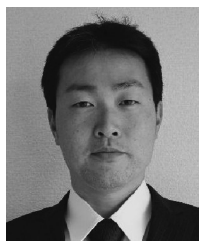
Financial supports such as Grant-in-Aid for Scientific Research and Global COE Program from Ministry of Education, Culture, Sports, Science and Technology (MEXT) Japan and Japan Society for the Promotion of Science (JSPS) are acknowledged.

References

- 1) T. J. Barton, L. M. Bull, W. G. Klemperer, D. A. Loy, B. McEnaney, M. Misono, P. A. Monson, G. Pez, G. W. Scherer, J. C. Vartuli and O. M. Yaghi, *Chem. Mater.*, 11, 2633–2656

- (1999).
- 2) J. Banhart, *Prog. Mater. Sci.*, **46**, 559–632 (2001).
 - 3) M. E. Davis, *Nature*, **417**, 813–821 (2002).
 - 4) S. Kitagawa, R. Kitaura and S. Noro, *Angew. Chem., Int. Ed.*, **43**, 2334–2375 (2004).
 - 5) A. R. Studart, U. T. Gonzenbach, E. Tervoort and L. J. Gauckler, *J. Am. Ceram. Soc.*, **89**, 1771–1789 (2006).
 - 6) J. Lee, J. Kim and T. Hyeon, *Adv. Mater.*, **18**, 2073–2094 (2006).
 - 7) C. J. Brinker and G. W. Scherer, in “Sol–Gel Science: The Physics and Chemistry of Sol–Gel Processing”, Academic Press, San Diego (1990).
 - 8) W. A. Braunecker and K. Matyjaszewski, *Prog. Polym. Sci.*, **32**, 93–146 (2007).
 - 9) K. Nakanishi and K. Kanamori, *J. Mater. Chem.*, **15**, 3776–3786 (2005).
 - 10) K. Kanamori and K. Nakanishi, *Chem. Soc. Rev.*, **40**, 754–770 (2011).
 - 11) K. Kanamori, *J. Ceram. Soc. Japan*, **119**, 16–22 (2011).
 - 12) K. Kanamori, *J. Sol-Gel Sci. Technol.*, submitted.
 - 13) H. D. Gesser and P. C. Goswami, *Chem. Rev.*, **89**, 765–788 (1989).
 - 14) J. Fricke and A. Emmerling, *J. Am. Ceram. Soc.*, **75**, 2027–2036 (1992).
 - 15) N. Hüsing and U. Schubert, *Angew. Chem., Int. Ed.*, **37**, 22–45 (1998).
 - 16) D. R. Rolison and B. Dunn, *J. Mater. Chem.*, **11**, 963–980 (2001).
 - 17) A. C. Pierre and G. M. Pajonk, *Chem. Rev.*, **102**, 4243–4265 (2002).
 - 18) B. E. Yoldas, M. J. Annen and J. Bostaph, *Chem. Mater.*, **12**, 2475–2484 (2000).
 - 19) H. Yokogawa and M. Yokoyama, *J. Non-Cryst. Solids*, **186**, 23–29 (1995).
 - 20) K. Kanamori, M. Aizawa, K. Nakanishi and T. Hanada, *Adv. Mater.*, **19**, 1589–1593 (2007).
 - 21) K. Kanamori, M. Aizawa, K. Nakanishi and T. Hanada, *J. Sol-Gel Sci. Technol.*, **48**, 172–181 (2008).
 - 22) K. Kanamori, K. Nakanishi and T. Hanada, *J. Ceram. Soc. Japan*, **117**, 1333–1338 (2009).
 - 23) S. S. Prakash, C. J. Brinker, A. J. Hurd and S. M. Rap, *Nature*, **374**, 439–443 (1995).
 - 24) F. Schwertfeger and D. F. M. Schmidt, *J. Non-Cryst. Solids*, **225**, 24–29 (1998).
 - 25) K. E. Parmenter and F. Milstein, *J. Non-Cryst. Solids*, **223**, 179–189 (1998).
 - 26) A. H. Alaoui, T. Woignier, G. W. Scherer and J. Phalippou, *J. Non-Cryst. Solids*, **354**, 4556–4561 (2008).
 - 27) K. Kanamori, Y. Kodera, G. Hayase, K. Nakanishi and T. Hanada, *J. Colloid Interface Sci.*, **357**, 336–344 (2011).
 - 28) K. Nakanishi, *J. Porous Mater.*, **4**, 67–112 (1997).
 - 29) K. Nakanishi and N. Tanaka, *Acc. Chem. Res.*, **40**, 863–873 (2007).
 - 30) K. Kanamori, H. Yonezawa, K. Nakanishi, K. Hirao and H. Jinnai, *J. Sep. Sci.*, **27**, 874–886 (2004).
 - 31) G. Hayase, K. Kanamori and K. Nakanishi, *J. Mater. Chem.*, **21**, 17077–17079 (2011).
 - 32) J. Livage, M. Henry and C. Sanchez, *Prog. Solid State Chem.*, **18**, 259–341 (1988).
 - 33) B. E. Yoldas, *J. Mater. Sci.*, **21**, 1087–1092 (1986).
 - 34) B. Yao and L. Zhang, *J. Mater. Sci.*, **34**, 5983–5987 (1999).
 - 35) H. Itoh, T. Tabata, M. Kokitsu, N. Okazaki, Y. Imizu and A. Tada, *J. Ceram. Soc. Japan*, **101**, 1081–1083 (1993).
 - 36) A. E. Gash, T. M. Tillotson, J. H. Satcher, Jr., J. F. Poco, L. W. Hrubesh and R. L. Simpson, *Chem. Mater.*, **13**, 999–1007 (2001).
 - 37) A. E. Gash, T. M. Tillotson, J. H. Satcher, Jr., L. W. Hrubesh and R. L. Simpson, *J. Non-Cryst. Solids*, **285**, 22–28 (2001).
 - 38) L. Chen, J. Zhu, Y.-M. Liu, Y. Cao, H.-X. Li, H.-Y. He, W.-L. Dai and K.-N. Fan, *J. Mol. Catal. A*, **255**, 260–268 (2006).
 - 39) G. Hasegawa, K. Kanamori, K. Nakanishi and T. Hanada, *J. Sol-Gel Sci. Technol.*, **53**, 59–66 (2010).
 - 40) G. Hasegawa, K. Kanamori, K. Nakanishi and T. Hanada, *J. Am. Ceram. Soc.*, **93**, 3110–3115 (2010).
 - 41) J. Konishi, K. Fujita, K. Nakanishi and K. Hirao, *Chem. Mater.*, **18**, 864–866 (2006).
 - 42) J. Konishi, K. Fujita, K. Nakanishi and K. Hirao, *Chem. Mater.*, **18**, 6069–6074 (2006).
 - 43) H. Matsuda, H. Nakamura and T. Nakajima, *Anal. Sci.*, **6**, 911–912 (1990).
 - 44) Y. Ikeguchi and H. Nakamura, *Anal. Sci.*, **16**, 541–543 (2000).
 - 45) G. Hasegawa, K. Morisato, K. Kanamori and K. Nakanishi, *J. Sep. Sci.*, **34**, 3004–3010 (2011).
 - 46) J. Konishi, K. Fujita, K. Nakanishi, K. Hirao, K. Morisato, S. Miyazaki and M. Ohira, *J. Chromatogr. A*, **1216**, 7375–7383 (2009).
 - 47) O. Ruzimuradov, G. Hasegawa, K. Kanamori and K. Nakanishi, *J. Am. Ceram. Soc.*, **94**, 3335–3339 (2011).
 - 48) O. Ruzimuradov, G. Hasegawa, K. Kanamori and K. Nakanishi, *J. Ceram. Soc. Japan*, **119**, 440–444 (2011).
 - 49) I. Gusev, X. Huang and C. Horváth, *J. Chromatogr. A*, **855**, 273–290 (1999).
 - 50) F. Svec, *J. Chromatogr. A*, **1217**, 902–924 (2010).
 - 51) W. A. Braunecker and K. Matyjaszewski, *Prog. Polym. Sci.*, **32**, 93–146 (2007).
 - 52) K. Matyjaszewski and J. Xia, *Chem. Rev.*, **101**, 2921–2990 (2001).
 - 53) C. J. Hawker, A. W. Bosman and E. Harth, *Chem. Rev.*, **101**, 3661–3688 (2001).
 - 54) M. Kamigaito, T. Ando and M. Sawamoto, *Chem. Rev.*, **101**, 3689–3745 (2001).
 - 55) G. Moad, E. Rizzardo and S. H. Thang, *Aust. J. Chem.*, **58**, 379–410 (2005).
 - 56) S. Yamago, *Chem. Rev.*, **109**, 5051–5068 (2009).
 - 57) T. Norisuye, T. Morinaga, Q. Tran-Cong-Miyata, A. Goto, T. Fukuda and M. Shibayama, *Polymer*, **46**, 1982–1994 (2005).
 - 58) Q. Yu, M. Zhou, Y. Ding, B. Jiang and S. Zhu, *Polymer*, **48**, 7058–7064 (2007).
 - 59) K. Kanamori, K. Nakanishi and T. Hanada, *Adv. Mater.*, **18**, 2407–2411 (2006).
 - 60) J. Hasegawa, K. Kanamori, K. Nakanishi, T. Hanada and S. Yamago, *Macromolecules*, **42**, 1270–1277 (2009).
 - 61) K. Kanamori, J. Hasegawa, K. Nakanishi and T. Hanada, *Macromolecules*, **41**, 7186–7193 (2008).
 - 62) G. Hasegawa, K. Kanamori, K. Nakanishi and S. Yamago, *Polymer*, **52**, 4644–4647 (2011).
 - 63) G. Hasegawa, K. Kanamori, K. Nakanishi, T. Hanada and S. Yamago, *Macromol. Rapid Commun.*, **30**, 986–990 (2009).
 - 64) C. Yu, M. H. Davey, F. Svec and J. M. J. Fréchet, *Anal. Chem.*, **73**, 5088–5096 (2001).
 - 65) K. Faure, M. Blas, O. Yassine, N. Delaunay, G. Crétier, M. Albert and J.-L. Rocca, *Electrophoresis*, **28**, 1668–1673 (2007).
 - 66) G. Proczek, V. Augustin, S. Descroix and M.-C. Hennion, *Electrophoresis*, **30**, 515–524 (2009).
 - 67) J. Hasegawa, K. Kanamori, K. Nakanishi and T. Hanada, *C. R. Chim.*, **13**, 207–211 (2010).
 - 68) G. Hasegawa, K. Kanamori, K. Nakanishi and T. Hanada, *Carbon*, **48**, 1757–1766 (2010).
 - 69) J. W. Neely, *Carbon*, **19**, 27–36 (1981).
 - 70) G. Hasegawa, M. Aoki, K. Kanamori, K. Nakanishi, T. Hanada and K. Tadanaga, *J. Mater. Chem.*, **21**, 2060–2063 (2011).
 - 71) C. Liang and S. Dai, *Chem. Mater.*, **21**, 2115–2124 (2009).
 - 72) A. Taguchi, J.-H. Smátt and M. Lindén, *Adv. Mater.*, **15**, 1209–1211 (2003).
 - 73) K. T. Lee, J. C. Lytle, N. S. Ergang, S. M. Oh and A. Stein, *Adv. Funct. Mater.*, **15**, 547–556 (2005).
 - 74) J. Pang, V. T. John, D. A. Loy, Z. Yang and Y. Lu, *Adv. Mater.*,

- 17, 704–707 (2005).
- 75) G. Hasegawa, K. Kanamori, K. Nakanishi and T. Hanada, *Chem. Commun. (Camb.)*, **46**, 8037–8039 (2010).
- 76) G. Hasegawa, K. Kanamori, K. Nakanishi and T. Hanada, *J. Mater. Chem.*, **19**, 7716–7720 (2010).
- 77) G. Hasegawa, K. Kanamori, K. Nakanishi and T. Hanada, *Chem. Mater.*, **22**, 2541–2547 (2010).
- 78) G. Hasegawa, K. Kanamori and K. Nakanishi, submitted.
- 79) R. Liu, Y. Shi, Y. Wan, Y. Meng, F. Zhang, D. Gu, Z. Chen, B. Tu and D. Zhao, *J. Am. Chem. Soc.*, **128**, 11652–11662 (2006).
- 80) H. Wei, Y. Lv, L. Han, B. Tu and D. Zhao, *Chem. Mater.*, **23**, 2353–2360 (2011).
-



Kazuyoshi Kanamori received Doctor of Engineering from Kyoto University in 2005. He was a Research Fellow of Japan Society for the Promotion of Science (JSPS) from 2004. After receiving the degree, he worked as a Postdoctoral Fellow of JSPS from 2005 to 2007. He is currently an Assistant Professor from 2007 at Department of Chemistry, Graduate School of Science, Kyoto University, Japan. His research interests are based on synthesis, characterization, and application of porous materials prepared via liquid-phase processes such as sol-gel and living polymerizations in polymer chemistry.
